

# $\beta$ -Strand Mimetic Foldamers Rigidified through Dipolar Repulsion\*\*

Elizabeth A. German, Jonathan E. Ross, Peter C. Knipe, Michaela F. Don, Sam Thompson,\* and Andrew D. Hamilton\*

**Abstract:** Many therapeutically relevant protein–protein interactions contain hot-spot regions on secondary structural elements, which contribute disproportionately to binding enthalpy. Mimicry of such  $\alpha$ -helical regions has met with considerable success, however the analogous approach for the  $\beta$ -strand has received less attention. Presented herein is a foldamer for strand mimicry in which dipolar repulsion is a central determinant of conformation. Computation as well as solution- and solid-phase data are consistent with an ensemble weighted almost exclusively in favor of the desired conformation.

The misregulation of protein–protein interactions (PPIs)<sup>[1]</sup> is implicated in many therapeutic areas, including HIV,<sup>[2]</sup> cancer,<sup>[3]</sup> diabetes,<sup>[4]</sup> and neurodegeneration.<sup>[5]</sup> To target these interactions there is a need for nonpeptidic mimics which are able to reproduce key distance and angular characteristics of protein surfaces.<sup>[6]</sup> Ideally, these scaffolds should be easily synthesized, stable under physiological conditions, and allow the display of a broad range of functional groups.

Since secondary structural motifs are often found at the interfacial regions of protein partners there has been extensive work in the field of nonpeptidic  $\alpha$ -helix mimicry.<sup>[7–12]</sup> There are also many examples in which an isolated  $\beta$ -strand (Figure 1 A) mediates an interaction between proteins,<sup>[13]</sup> yet  $\beta$ -strand mimicry remains relatively unexplored.<sup>[14–16]</sup> Possible peptidomimetic solutions should allow controlled positioning of side-chain functionality on specific vectors above and below a planar scaffold, as well as facile extension in a modular fashion to permit mimicry of larger surfaces.

Previous work in our group has focused on the mimicry of one recognition surface of the strand—that presenting the  $i$ ,  $i+2$ , and  $i+4$  side-chain residues. Earlier-generation scaffolds have included 2,2-disubstituted-indolin-3-ones<sup>[17]</sup> and aryl-linked hydantoins.<sup>[15]</sup> However, the development of these approaches was hindered by the need for asymmetric syntheses of all-carbon quaternary centers.

Recent work obviates this problem with the use of oligomers of alternating aryl-linked imidazolidin-2-ones, which are easily assembled from amino-acid derivatives (Figure 1 B).<sup>[16]</sup> In solution this scaffold undergoes relatively free rotation around the  $C_{\text{aryl}}-N_{\text{urea}}$  single bonds and interconverts among at least three principal conformers, thus likely requiring an induced-fit mode of protein binding (Figure 1 B, structures I–III). Therefore we sought to impart conformational control on this system through replacement of the phenyl linkers with pyridines. This new linker should retain the shape and planarity of the previous scaffold but also impart conformational bias through dipolar repulsion. A molecular mechanics calculation<sup>[18]</sup> on the extent of bias gave an energy profile for the rotation about the  $C_{\text{pyr}}-N_{\text{urea}}$  bond relative to the equivalent bond in the previous scaffold. For the pyridyl model this corresponds to 98 % of the populated

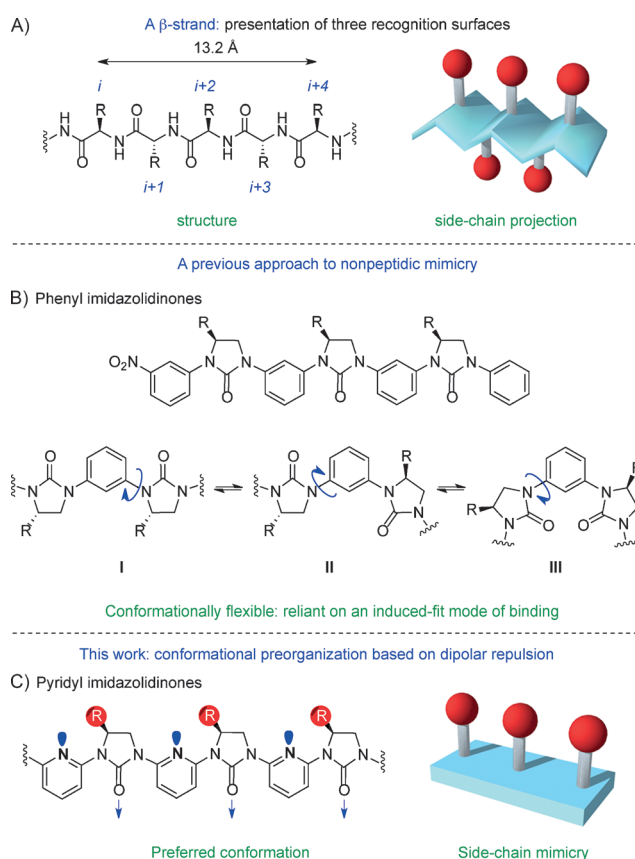


**Figure 1.** A nonpeptidic approach to  $\beta$ -strand mimicry. A) Schematic representation of a  $\beta$ -strand, and a pegboard representation showing side-chain projection. B) Previous work: aryl-linked imidazolidin-2-ones. C) This work: a 2,6-pyridyl-linked imidazolidin-2-one with dipole repulsion designed to impart conformational bias.

[\*] E. A. German, J. E. Ross, Dr. P. C. Knipe, M. F. Don, Dr. S. Thompson, Prof. Dr. A. D. Hamilton  
Chemistry Research Laboratory, University of Oxford  
12 Mansfield Road, Oxford, OX1 3TA (UK)  
E-mail: sam.thompson@chem.ox.ac.uk  
andrew.hamilton@chem.ox.ac.uk  
Homepage: <http://hamilton.chem.ox.ac.uk>

[\*\*] We thank the EPSRC (EP/G03706X/1) and The University of Oxford for funding, Dr. Amber L. Thompson for assistance with X-ray crystallography and Diamond Light Source for an award of beamtime (MT9981).

Supporting information for this article is available on the WWW under <http://dx.doi.org/10.1002/anie.201410290>.

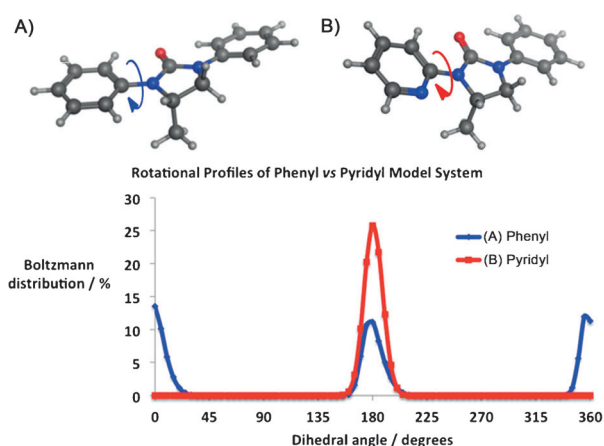


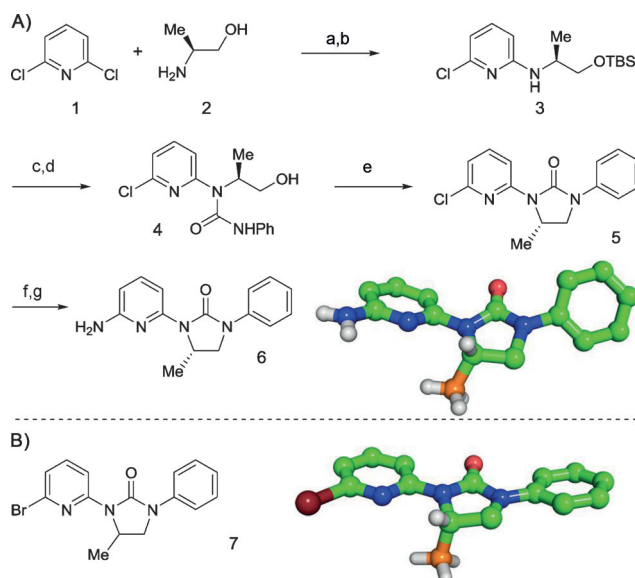
**Figure 2.** Computed room-temperature Boltzmann-weighted populations of A) phenyl and B) pyridyl systems as a function of dihedral angle.

conformations being within  $\pm 15$  degrees of the planar conformation in which the dipoles are perfectly opposed (Figure 2).

With computational support in hand we sought proof of principle through the mimicry of three alanine side chains. Nucleophilic aromatic substitution of 2,6-dichloropyridine (**1**) with L-alaninol (**2**) gave an amino alcohol in 82 % yield<sup>[19]</sup> and subsequent *O*-silylation with a TBS group gave **3** (Scheme 1A). Deprotonation of the amine and reaction of the resultant anion with phenyl isocyanate proceeded to give the urea in 68 % yield. Desilylation to afford **4**, followed by an intramolecular Mitsunobu reaction gave the imidazolidin-2-one monomer **5** in 62 % yield over two steps.<sup>[16]</sup> Buchwald–Hartwig coupling with benzylamine<sup>[20]</sup> and subsequent treatment with hydrogen and Pearlman's catalyst unmasked the aniline **6** in good yield. The conformations of **6** and **7** (generated racemically by an analogous route; see the Supporting Information for full details) were examined by single-crystal X-ray diffraction (Scheme 1).<sup>[21]</sup> Both were found to adopt the conformation expected on the basis of dipolar repulsion, with  $N_{\text{pyr}}\text{--C--N--C}_{\text{urea}}$  dihedral angles of  $143^\circ$  and  $175^\circ$  respectively. The amine **6** may be less planar than **7** because of the increased pyridine electron density, which reduces its  $\pi$  conjugation with the urea. In both cases the side-chain methyl groups are projected into pseudoaxial positions by the puckered imidazolidinone rings, in a manner analogous to the projection of side-chains by natural  $\beta$ -strands.

Deprotonation of the secondary amine **3** with *n*BuLi and trapping with phenyl chloroformate gave the carbamate **8** in 84 % yield (Scheme 2A). The compound **8** was then coupled with the lithium anilide of **6** to give the intermediate urea, which following TBAF-mediated deprotection and cyclization, afforded the two-residue mimic **9**. Further iteration on **9** of this amination, coupling with **8**, and a cyclization sequence afforded the three-residue mimic **10** (Scheme 2B; see the Supporting Information).

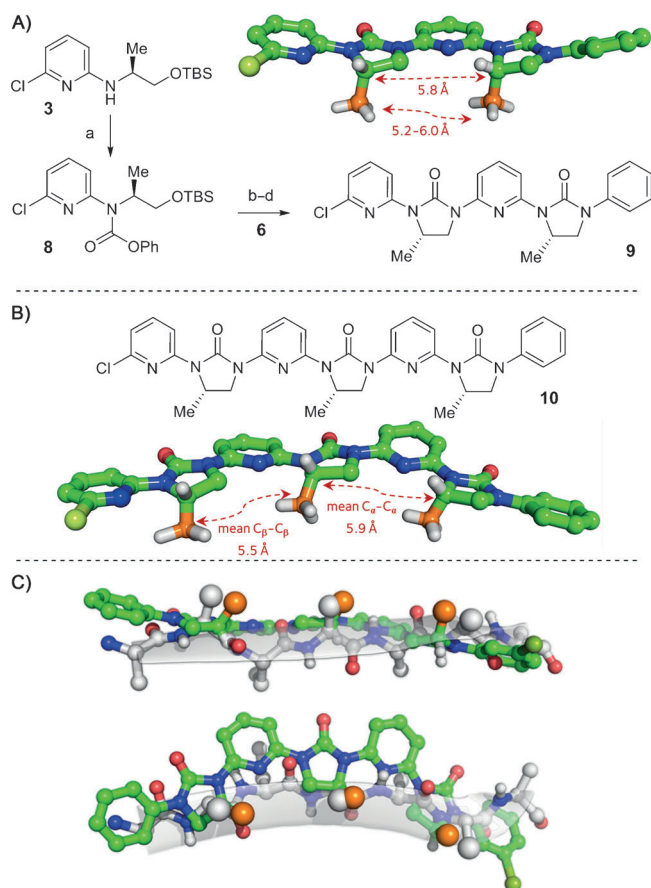
Single-crystal X-ray structures were obtained for **9** and **10**.<sup>[21]</sup> For **9** two different structures were present within the asymmetric unit (Scheme 2A). As a consequence of dipolar repulsion, both present the side-chains on the same face of the



**Scheme 1.** A) Reagents and conditions: a) DIPEA,  $180^\circ\text{C}$ , sealed tube, 82 %; b) TBSCl, imidazole, DMAP (cat.), DMF, 99 %; c) *n*BuLi, THF; then PhNCO, 68 %; d) TBAF,  $\text{CH}_3\text{CO}_2\text{H}$ , THF, 78 %; e)  $\text{PPh}_3$ , DIAD, THF, 79 %; f)  $[\text{Pd}_2(\text{dba})_3]$ , ( $\pm$ )-binap, NaOtBu,  $\text{H}_2\text{NCH}_2\text{Ph}$ , 1,4-dioxane, 95 %; g)  $\text{Pd}(\text{OH})_2/\text{C}$ ,  $\text{H}_2$ ,  $\text{CH}_3\text{CO}_2\text{H}$ ,  $\text{CH}_2\text{Cl}_2$ , 86 %. X-Ray diffraction structures of monomers (side-chains highlighted in orange, some hydrogen atoms omitted for clarity) **6**. B) ( $\pm$ )-**7** (with molecular structure, left. The *S* enantiomer was chosen arbitrarily). binap = 2,2'-bis(diphenylphosphanyl)-1,1'-binaphthyl, dba = dibenzylideneacetone, DIAD = diisopropylazodicarboxylate, DIPEA = diisopropylethylamine, DMAP = 4-(*N,N*-dimethylamino)pyridine, DMF = *N,N*-dimethylformamide, TBAF = tetra-*n*-butylammonium fluoride, TBS = *tert*-butyldimethylsilyl, THF = tetrahydrofuran.

molecule, with the  $\alpha$ -carbon atoms 5.8 Å and the  $\beta$ -carbon atoms 6.0 Å and 5.2 Å apart; the distances are within the range of those in natural  $\beta$ -strands. The crystal structure of **10** exhibited similar conformational preferences, with the methyl side-chains projected from the same face of an approximately planar scaffold. As with the dimer, two molecules of **10** were present in the asymmetric unit, with mean  $\alpha$ -carbon and  $\beta$ -carbon separations of 5.9 Å and 5.5 Å, respectively (Scheme 2B). For **6**, **7**, **9** and **10**, the conformation of all pyridyl–urea linkages exclusively placed the pyridine nitrogen atom *anti* to the urea carbonyl group. This placement suggests that dipolar repulsion is effective as a key determinant for global conformation. Comparison of the X-ray crystal structure of **10** with a natural  $\beta$ -strand revealed good overlap of strand  $C_\alpha$  and  $C_\beta$  positions with the equivalent groups on the mimic, with a six-point RMSD of 1.1 Å (Scheme 2C).

NMR experiments were conducted to provide insight into the solution-phase conformational behavior (Figure 3). NOESY analysis of **9** revealed an extremely weak correlation between H12 and H14, indicating that the illustrated conformation is the primary one. It is conceivable that the observed weak crosspeak is a consequence of: 1) a small degree of conformational flexibility allowing access to a conformer resembling **II** (Figure 1B), with the low intensity reflecting its low population; or 2) complete conformational rigidity. The distance between H12 and H14 (see crystal structure) is 4.5 Å, which is on the edge of detection for the



**Scheme 2.** A) Two-residue mimic **9**. Reagents and conditions: a) *n*BuLi, PhCOCl, THF,  $-78^{\circ}\text{C}$ , 84%; b) *n*BuLi, **6**, THF,  $-78^{\circ}\text{C}$ , 48%; c) TBAF,  $\text{CH}_3\text{CO}_2\text{H}$ , THF, 81%; d)  $\text{PPh}_3$ , DIAD, THF, 75%. B) Three-residue mimic **10**. See the Supporting Information for synthesis. X-ray diffraction structures with side-chains highlighted in orange (some hydrogen atoms omitted for clarity). C) Overlay of mimic (green) with natural  $\beta$ -strand (gray; extracted from PDB 3QXT, side-chains truncated for clarity), with six-point ( $\alpha$ - and  $\beta$ -carbon atoms) RMSD of 1.1 Å.

nOe effect, but may be sufficiently short to give some weak correlation. A semiquantitative measure for the significance of these nOe results can be obtained by comparison with the H3–H5 crosspeak. In the absence of any conformational controlling effects, the expected nOe intensity of the H3–H5 crosspeak would be approximately twice that of the H12–H14 peak (because of the  $\text{C}_2$  symmetry of the phenyl group). The observed relative intensity of nOe signals (obtained by integration of the NOESY spectrum) is 39:1, suggesting an approximate 20:1 relative intensity of through-space interactions. The same behavior is exhibited by the trimer **10**: H12–H14 and H21–H23 NOESY crosspeaks have much lower intensity than the internal control H3–H5 correlation. Because of the spectral coincidence between the crosspeaks these could not be integrated individually, but the ratio between the reference H3–H5 and the combined H12–H14 and H21–H23 crosspeaks was 18:1, thus indicating an average 18:1 relative intensity of through-space interactions. These solution-state results are in good agreement with the initial premise of dipole-enforced conformational control, and with

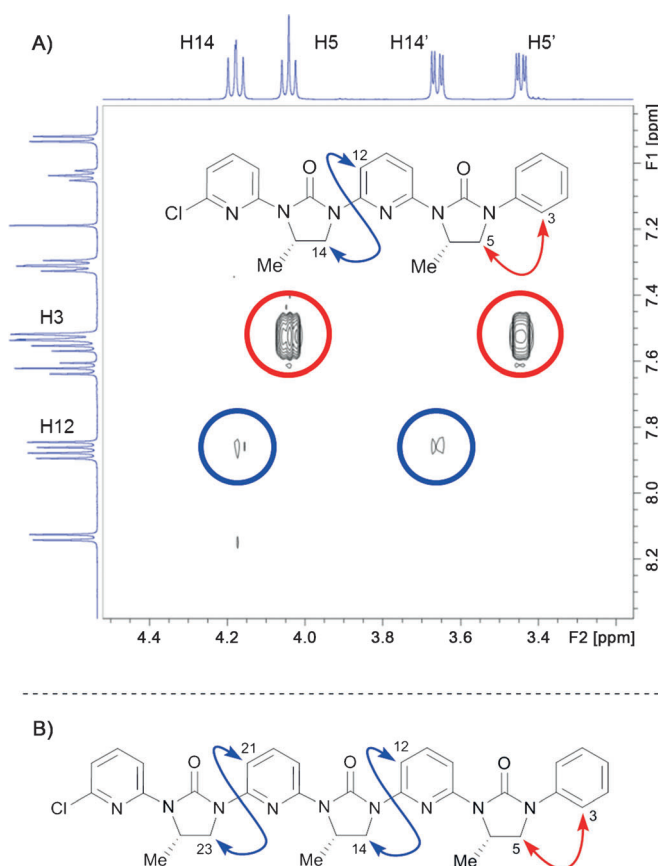


**Figure 3.** A) Selected regions of NOESY spectrum for the two-residue mimic **9**. Arrows indicate relevant nOe correlations, with those in blue indicating weak interactions and those in red strong interactions (500 MHz,  $\text{CDCl}_3$ , 0.02 mM, see the Supporting Information for larger versions). B) nOe correlations for the three-residue mimic **10** (600 MHz,  $\text{CDCl}_3$ ).

the X-ray crystallographic analysis. These data indicate that in solution as well as in the solid state the side-chains are indeed projected uniformly from a single face of the  $\beta$ -strand mimetic, in the same manner as that of the side-chains in natural  $\beta$ -sheets and  $\beta$ -strands.

In conclusion we have designed and synthesized a non-peptidic scaffold capable of mimicking a recognition surface of a  $\beta$ -strand (in this case the side-chains of the  $i$ ,  $i+2$ , and  $i+4$  residues). Computation as well as solid- and solution-phase studies are consistent with the population of an ensemble in which the desired conformation is heavily biased by dipolar repulsion. The synthesis is modular, scalable, and amenable to the incorporation of a wide variety of side-chains, including those with no proteinogenic congener. Work is underway in our laboratory to prepare mimics of therapeutically relevant  $\beta$ -strands using this scaffold, and to further exploit dipolar repulsion to exert conformational control over related systems.

Received: October 20, 2014

Published online: January 19, 2015

**Keywords:** peptidomimetics · protein–protein interactions · protein structures · solid-state structures · synthetic methods

- 
- [1] S. Jones, J. M. Thornton, *Proc. Natl. Acad. Sci. USA* **1996**, *93*, 13.  
 [2] A. Tavassoli, *Chem. Soc. Rev.* **2011**, *40*, 1337.  
 [3] A. A. Ivanov, F. R. Khuri, H. Fu, *Trends Pharmacol. Sci.* **2013**, *34*, 393.  
 [4] A. Sharma, S. Chavali, A. Mahajan, R. Tabassum, V. Banerjee, N. Tandon, D. Bharadwaj, *Mol. Cell. Proteomics* **2005**, *4*, 1029.  
 [5] J. Goñi, F. J. Esteban, N. V. de Mendizábal, J. Sepulcre, S. Ardanza-Trevijano, I. Agirrezabal, P. Villoslada, *BMC Syst. Biol.* **2008**, *2*, 52.  
 [6] M. R. Arkin, J. A. Wells, *Nat. Rev. Drug Discovery* **2004**, *3*, 301.  
 [7] V. Azzarito, K. Long, N. S. Murphy, A. J. Wilson, *Nat. Chem.* **2013**, *5*, 161.  
 [8] M. K. P. Jayatunga, S. Thompson, A. D. Hamilton, *Bioorg. Med. Chem. Lett.* **2013**, *24*, 717.  
 [9] O. V. Kulikov, S. Thompson, H. Xu, C. D. Incarvito, R. T. W. Scott, I. Saraogi, L. Nevola, A. D. Hamilton, *Eur. J. Org. Chem.* **2013**, 3433.  
 [10] S. Thompson, A. D. Hamilton, *Org. Biomol. Chem.* **2012**, *10*, 5780.  
 [11] P. Tošovská, P. S. Arora, *Org. Lett.* **2010**, *12*, 1588.  
 [12] S. Marimnganti, M. N. Cheemala, J.-M. Ahn, *Org. Lett.* **2009**, *11*, 4418.  
 [13] H. Remaut, G. Waksman, *Trends Biochem. Sci.* **2006**, *31*, 436.  
 [14] W. A. Loughlin, J. D. A. Tyndall, M. P. Glenn, T. A. Hill, D. P. Fairlie, *Chem. Rev.* **2010**, *110*, PR32.  
 [15] A. G. Jamieson, D. Russell, A. D. Hamilton, *Chem. Commun.* **2012**, 48, 3709.  
 [16] C. L. Sutherell, S. Thompson, R. T. W. Scott, A. D. Hamilton, *Chem. Commun.* **2012**, 48, 9834.  
 [17] P. N. Wyrembak, A. D. Hamilton, *J. Am. Chem. Soc.* **2009**, *131*, 4566.  
 [18] Chemical Computing Group, Inc., *Molecular Operating Environment (MOE)*, Montreal, QC, Canada, **2013**.  
 [19] A. Faust, O. Wolff, S. R. Waldvogel, *Synthesis* **2009**, 155.  
 [20] A. D. Averin, O. A. Ulanovskaya, A. A. Borisenko, M. V. Serebryakova, I. P. Beletskaya, *Tetrahedron Lett.* **2006**, *47*, 2691.  
 [21] CCDC 1030066 (**6**), 1030067 (**7**), 1030068 (**9**), and 1030069 (**10**) contain the supplementary crystallographic data for this paper. These data can be obtained free of charge from The Cambridge Crystallographic Data Centre via [www.ccdc.cam.ac.uk/data\\_request/cif](http://www.ccdc.cam.ac.uk/data_request/cif).
-